Antenna Tilt Optimization for Multi-Cell Massive MIMO Systems with Two Tilts

Deming Chu and Anzhong Hu

***Abstract*—In this paper, we study the optimization of two tilt angles corresponding to two antenna arrays in each base station (BS) of a massive multiple-input multiple-output system. We consider two scenarios with perfect channel state information (CSI) and imperfect CSI. In the limit of the number of the BS antennas, the channel orthogonality is employed to derive the limit and the lower bound of the throughputs. By maximizing the lower bound or the limit throughput, the two antenna tilt angles are optimized. Simulation results show that the throughput performance can be improved with the designed tilt angles.**

***Index Terms*—massive MIMO, 5G, tilt, channel estimation, throughput**

I. Introduction

Massive multiple-input multiple-output (MIMO) is the key technology to improve system capacity and spectral efficiency in the fifth generation mobile communication, thus has been widely used. However, one of the fundamental factors limiting the performance of a multi-cell massive MIMO system is the inter-cell interference (ICI), especially for the users at the cell-edge. In order to mitigate the interference in massive MIMO systems, several methods have been proposed [1]-[3]. However, these methods do not consider antenna gain in the vertical direction.

Antenna tilt angle, which is later referred to as tilt, is the elevation angle of the antenna pattern, and can be adjusted to control the antenna gain. Thus, the effect between signal and interference can be effectively balanced by optimizing the antenna tilt in multi-cell massive MIMO systems. There are two types of tilt, i.e., the mechanical tilt and the electrical tilt. Mechanical tilt is a physical downward tilt of a directional antenna. Its construction and maintenance are very cumbersome, and the accuracy of adjusting the tilt angle is low (step accuracy is 1°). The electrical tilt is adjusted by changing the phase shifts of the antenna array. Moreover, the electrical tilt can be dynamically adjusted with high accuracy (step accuracy is 0.1°).

The tilt of base station antennas has been extensively studied in cellular systems [4]-[8]. In [4], the electrical tilts are jointly adjusted to maximize the throughput with the availability of the location information of the scheduled users. The work in [5] divides the coverage area into two vertical regions, and then optimizes the mechanical tilt to serve the users in each vertical region. In [6], the antenna tilt is adjusted to maximize the sum rate in a single cell MIMO system. In [7], the cell is divided into two sectors in vertical direction, and the base station (BS) is configured with two antenna arrays corresponding to two antenna tilts. Then, two tilts, user scheduling, and resource block allocation are considered. However, the ICI and multiple tilts are not jointly considered in these papers.

To exploit the degrees of freedom of the channel in the elevation direction, the horizontal and the vertical beam pattern adaptation (i.e., three dimensional (3D) beamforming) technology has been proposed in recent years [9]-[11]. The optimal beam angles for the 3D antenna systems are studied based on the probability density functions of the 3D user distribution in [9]. In [10], the 3D beamforming is exploited to provide additional degrees of freedom to avoid the ICI in laboratory and field test setups. Coordinated 3D beamforming is proposed in [11], which jointly adapts the beamforming in the horizontal plane and the mechanical tilts in the vertical plane to control the ICI. However, these methods are only feasible with the perfect channel state information (CSI).

In this paper, an antenna tilt optimization method for multi-cell massive MIMO systems is proposed to maximize the cell throughput. We study a transmission framework that the BS is equipped with two linear arrarys parallel to the ground, which correspond to two mechanical tilts, respectively. In the case that the number of the BS antennas tends to infinity, we get the optimal tilts by maximizing the throughput with perfect CSI and imperfect CSI scenarios. In this paper, we makes the following specific contributions:

- We derive the asymptotic expression of the throughput for the multi-cell massive MIMO system with the number of the base station antennas tends to infinity. At the BS side, we set it to have two antenna arrays corresponding to two tilts, which can cover two sector areas. In contrast, they only study one tilt or the single-cell system in [4]-[7].
- We study the expressions of the throughput in two scenarios with the perfect CSI and imperfect CSI, respectively. In the case of the imperfect CSI, both the intra-cell interference and ICI should be considered. However, they only study with the perfect CSI in [9]-[11].
- The throughput limit or the throughput lower bound derived are functions of the user distributions. Hence, it is convenient to obtain the two optimal tilts by maximizing the throughput limit or the throughput lower bound. Simulation results show that the proposed approach can enhance the throughput of the cell with two mutually coordinated antenna tilts compared to conventional systems.

The rest of the paper is organized as follows. In Section II, we describe the multi-cell massive MIMO system model and the

D. Chu and A. Hu are with the School of Communication Engineering, Hangzhou Dianzi University, Hangzhou 310018, China, e-mail: 1980203958@qq.com, huaz@hdu.edu.cn. A. Hu is the corresponding author.

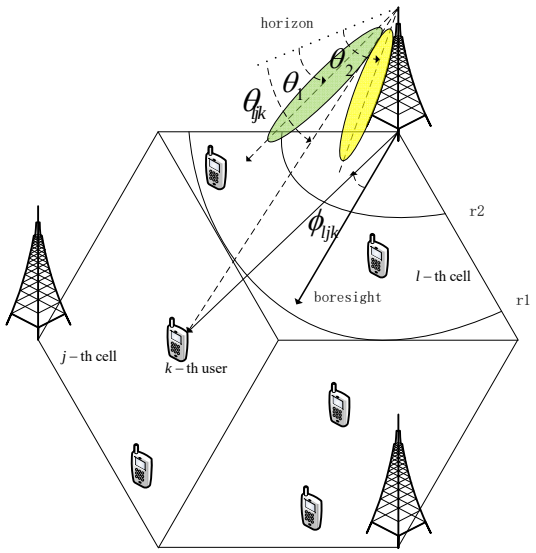

Fig. 1. A cellular layout example with $L = 3, K = 2$.

propagation environment. In Sections III and IV, we analyze the throughputs in two scenarios with the perfect CSI and the imperfect CSI, respectively. Section V shows the numerical results. We conclude the paper in Section VI.

Notations: Lower-case (upper-case) boldface symbols denote vectors (matrices); $\mathbf{I}_K$ represents the $K \times K$ identity matrix; $\mathrm{Tr}(\cdot)$, $(\cdot)^H$, and $|\cdot|$ denote the trace operator, the conjugate transpose, and the absolute value, respectively; $\mathbf{0}_K$ represents the $K \times 1$ zero vector; $\mathbb{E}\{\cdot\}$ denotes the expectation; $\|\mathbf{x}\|$ denotes the Euclidean 2-norm of a complex vector $\mathbf{x}$; $\mathrm{diag}\{a_1, \cdots, a_K\}$ represents a K dimensional diagonal matrix with the k-th diagonal element a_k; $\delta(\cdot)$ is the delta function; $\mathbf{e}_k$ denotes the standard basis vector with the k-th element being 1; $\mathbf{z} \sim \mathcal{CN}(\boldsymbol{\mu}, \boldsymbol{\Sigma})$ means that $\mathbf{z}$ is a complex circularly symmetric Gaussian vector with mean $\boldsymbol{\mu}$ and covariance matrix $\boldsymbol{\Sigma}$; $[\mathbf{a}]_k$ and $[\mathbf{A}]_k$ denote the k-th element of the vector $\mathbf{a}$ and the k-th column vector of the matrix $\mathbf{A}$, respectively.

II. System Model

We consider the downlink transmission in a network consisting of L mutually interfering cells. The system operates in time division duplex mode and in the block fading scenario. Moreover, the cell radius is denoted as r_1 and the cell hole radius is denoted as r_2. There are K single antenna users distributed uniformly in each cell with $r_1 \leq d \leq r_2$, where d is the distance between one user and the BS foot in the same cell. Each BS is equipped with two linear arrays parallel to the ground with the boresight to the center of the cell. The two arrays are equipped with M_1 antennas and M_2 antennas, respectively. In Fig. 1, a 3-cell network is illustrated. The BS height is h_{BS}. The tilts for the antenna elements in the same array are identical.

The radiation pattern for the BS array with M_1 antennas in the l-th cell for the k-th user in the j-th cell follows the model proposed by 3GPP and is defined (in dBi scale) as [12]

$$\tilde{\alpha}_{ljk}(\theta_1) = -\min\left(\min\left[12\left(\frac{\phi_{ljk}}{\phi_{3\mathrm{dB}}}\right)^2, SLL_{\mathrm{az}}\right] + \min\left[12\left(\frac{\theta_{ljk}-\theta_1}{\theta_{3\mathrm{dB}}}\right)^2, SLL_{\mathrm{el}}\right], SLL_{\mathrm{tot}}\right) + \alpha_{\max}, \quad (1)$$

where ϕ_{ljk} denote the azimuth angle measured between the line in the azimuth plane connecting the k-th user in the j-th cell to the BS in the l-th cell and the array boresight, and ϕ_{ljk} is positive for counter-clockwise direction; θ_{ljk} is the elevation angle measured between the line connecting the k-th user in the j-th cell to the BS in the l-th cell and the horizontal plane, θ_{ljk} is positive if the line is below the horizon; θ_1 denotes the mechanical tilt of the BS array with M_1 antennas. Moreover, $\phi_{3\mathrm{dB}}$ and $\theta_{3\mathrm{dB}}$ denote the half-power beamwidth in the azimuth and the elevation pattern, respectively, SLL_{az} and SLL_{el} are the side lobe levels for the respective patterns, and SLL_{tot} denotes the total side lobe level. $\alpha_{\max}$ denotes the highest gain of the antenna. Similarly, the radiation pattern for the BS array with M_2 antennas in the l-th cell for the k-th user in the j-th cell is denoted as $\tilde{\alpha}_{ljk}(\theta_2)$, where θ_2 denotes the mechanical tilt of the BS array with M_2 antennas. Then, we have the effective antenna gain as

$$\alpha_{ljk}(\theta_1) = \tilde{\alpha}_{ljk}(\theta_1)\,\beta_{ljk}, \quad (2)$$

where β_{ljk} denotes the large scale fading from the BS of the l-th cell to the k-th user of the j-th cell. Similarly, we can get $\alpha_{ljk}(\theta_2) = \tilde{\alpha}_{ljk}(\theta_2)\,\beta_{ljk}$.

The complex baseband discrete time signal received at the k-th user of the j-th cell is given by

$$y_{jk} = \mathbf{h}_{jjk}^H \mathbf{s}_j + \sum_{j' \neq j} \mathbf{h}_{j'jk}^H \mathbf{s}_{j'} + n_{jk}, \quad (3)$$

where $n_{jk} \sim \mathcal{CN}(0, \sigma_{\mathrm{n}}^2)$ is the noise received at the k-th user of the j-th cell, $\mathbf{s}_j \in \mathbb{C}^{\mathrm{M}\times 1}$ is the transmitted signal of the j-th cell, and $\mathbf{h}_{ljk} \in \mathbb{C}^{\mathrm{M}\times 1}$ is the channel between the user k of the j-th cell and the BS l. The transmitted signal vector can be expressed as

$$\mathbf{s}_j = \sqrt{\rho_j}\mathbf{F}_j \mathbf{d}_j, \quad (4)$$

where ρ_j denotes power factor (i.e., power amplification); $\mathbf{F}_j \in \mathbb{C}^{\mathrm{M}\times \mathrm{K}}$ denotes the transmit beamforming matrix and $\mathbf{d}_j \in \mathbb{C}^{\mathrm{K}\times 1}$ denotes the data symbol vector intended for the K users in the j-th cell. Additionally, we have

$$\mathbb{E}\{\mathbf{d}_j \mathbf{d}_j^H\} = \mathbf{I}_K, \quad (5)$$

and the transmission power of the j-th BS is

$$P_j = \mathbb{E}\left\{\|s_j\|^2\right\}. \quad (6)$$

In (4) and (6), ρ_j varies with F_j to ensure that P_j is constant. Then, P_j/K is a constant, i.e., the power to each user is a constant like [13]. We represent the channel vector as

$$\mathbf{h}_{ljk} = \begin{bmatrix} \alpha_{ljk}(\theta_1)\mathbf{h}_{ljk1} \\ \alpha_{ljk}(\theta_2)\mathbf{h}_{ljk2} \end{bmatrix}, \quad (7)$$

where $\mathbf{h}_{ljk1} \in \mathbb{C}^{M_1\times 1}$ and $\mathbf{h}_{ljk2} \in \mathbb{C}^{M_2\times 1}$ denote the channel vectors for M_1 antenna array and M_2 antenna array, respectively. We assume that $\mathbf{h}_{ljk1} \sim \mathcal{CN}(\mathbf{0}_{M_1}, \mathbf{I}_{M_1})$ and $\mathbf{h}_{ljk2} \sim \mathcal{CN}(\mathbf{0}_{M_2}, \mathbf{I}_{M_2})$.

Then, we substitute (4) into (3) and rewrite the expression for the received signal as

$$\begin{aligned} y_{jk} &= \sqrt{\rho_j}\mathbf{h}_{jjk}^H\mathbf{F}_j\mathbf{d}_j + \sum_{j'\neq j}\sqrt{\rho_{j'}}\mathbf{h}_{j'jk}^H\mathbf{F}_{j'}\mathbf{d}_{j'} + n_{jk} \\ &= \sqrt{\rho_j}\mathbf{h}_{jjk}^H[\mathbf{F}_j]_k[\mathbf{d}_j]_k + \sum_{k'\neq k}\sqrt{\rho_j}\mathbf{h}_{jjk}^H[\mathbf{F}_j]_{k'}[\mathbf{d}_j]_{k'} \\ &\quad + \sum_{j'\neq j}\sqrt{\rho_{j'}}\mathbf{h}_{j'jk}^H\mathbf{F}_{j'}\mathbf{d}_{j'} + n_{jk}, \end{aligned} \tag{8}$$

where the middle two items denote the intra-cell interference and the ICI, respectively. Then, the signal-to-interference-plus-noise ratio (SINR) of the k-th user in the j-th cell is denoted as (9).

The corresponding ergodic throughput for all the K users in the j-th cell can be expressed as

$$R_j(\theta_1,\theta_2) = K\mathbb{E}\left\{\log_2\left(1+\gamma_{jk}(\theta_1,\theta_2)\right)\right\}, \tag{10}$$

where the expectation is taken with respect to the effective antenna gain. In this paper, our ultimate goal is to obtain the two tilts θ_1 and θ_2 by maximizing the throughput $R_j(\theta_1,\theta_2)$. Thus, the optimization problem can be formulated as

$$\max_{\theta_1,\theta_2} R_j(\theta_1,\theta_2). \tag{11}$$

Next, we will study (11) in two scenarios, i.e., the system with the perfect CSI and the imperfect CSI.

III. Optimization for the Perfect CSI

In this section, we will develop the solution to (11) with the perfect CSI. We first derive the expression of SINR containing the signal power. Then, we analysis the signal power in (6). Finally, we get the asymptotic expression of the throughput in the asymptotic case, and obtain the two tilts by maximizing the expression.

A. Analysis of the SINR

To cancel the intra-cell interference, we focus on linear zero-forcing beamforming. We assume perfect CSI of all the users in each cell is available at the BS. Since zero-forcing precoders are considered, we have

$$\mathbf{F}_j = \mathbf{H}_{jj}\left(\mathbf{H}_{jj}^H\mathbf{H}_{jj}\right)^{-1}, \tag{12}$$

where $\mathbf{H}_{jj} = [\mathbf{h}_{jj1}\mathbf{h}_{jj2}\cdots\mathbf{h}_{jjk}\cdots\mathbf{h}_{jjK}] \in \mathbb{C}^{\mathrm{M}\times\mathrm{K}}$ denotes the channel matrix from the j-th BS to the K users in the j-th cell. Then, (8) can be re-expressed as

$$y_{jk} = \sqrt{\rho_j}[\mathbf{d}_j]_k + \sum_{j'\neq j}\sqrt{\rho_{j'}}\mathbf{h}_{j'jk}^H\mathbf{F}_{j'}\mathbf{d}_{j'} + n_{jk}. \tag{13}$$

We can now write the SINR of the k-th user in the j-th cell as

$$\begin{aligned} \gamma_{jk}(\theta_1,\theta_2) &= \frac{\mathbb{E}\left\{\left|\sqrt{\rho_j}[\mathbf{d}_j]_k\right|^2\right\}}{\mathbb{E}\left\{\sum_{j'\neq j}\left|\sqrt{\rho_{j'}}\mathbf{h}_{j'jk}^H\mathbf{F}_{j'}\mathbf{d}_{j'}\right|^2 + \sigma_{\mathrm{n}}^2\right\}} \\ &= \frac{\rho_j}{\sum_{j'\neq j}\rho_{j'}\left\|\mathbf{h}_{j'jk}^H\mathbf{H}_{j'j'}\left(\mathbf{H}_{j'j'}^H\mathbf{H}_{j'j'}\right)^{-1}\right\|^2 + \sigma_{\mathrm{n}}^2}, \end{aligned} \tag{14}$$

where the second equation is based on (5).

To further simplify the SINR expression, we will analyze in the asymptotic region.

Lemma 1. *Assume that M, M_1, and M_2 satisfy $M_1/M = \eta$, $M_2/M = 1-\eta$, then when taking the limit, (14) can be expressed as*

$$\bar{\gamma}_{jk}(\theta_1,\theta_2) = \lim_{M\to\infty}\gamma_{jk}(\theta_1,\theta_2) = \frac{\rho_j}{\sigma_{\mathrm{n}}^2}. \tag{15}$$

Proof: We first analyze each item on the denominator on (14).

1) For $\mathbf{H}_{j'j'}^H\mathbf{H}_{j'j'}$, we have

$$\begin{aligned} &\mathbf{h}_{j'j'k}^H\mathbf{h}_{j'j'k'} \\ &= \begin{bmatrix} \alpha_{j'j'k}(\theta_1)\mathbf{h}_{j'j'k1} \\ \alpha_{j'j'k}(\theta_2)\mathbf{h}_{j'j'k2} \end{bmatrix}^H \begin{bmatrix} \alpha_{j'j'k'}(\theta_1)\mathbf{h}_{j'j'k'1} \\ \alpha_{j'j'k'}(\theta_2)\mathbf{h}_{j'j'k'2} \end{bmatrix} \\ &= \alpha_{j'j'k}^*(\theta_1)\alpha_{j'j'k'}(\theta_1)\mathbf{h}_{j'j'k1}^H\mathbf{h}_{j'j'k'1} \\ &\quad + \alpha_{j'j'k}^*(\theta_2)\alpha_{j'j'k'}(\theta_2)\mathbf{h}_{j'j'k2}^H\mathbf{h}_{j'j'k'2}. \end{aligned}$$

When the number of the BS antennas tends to infinity, for $\mathbf{h}_{j'j'k1}^H\mathbf{h}_{j'j'k'1}$ and $\mathbf{h}_{j'j'k2}^H\mathbf{h}_{j'j'k'2}$, we have

$$\begin{aligned} \lim_{M\to\infty}\frac{1}{M}\mathbf{h}_{j'j'k1}^H\mathbf{h}_{j'j'k'1} &= \eta\lim_{M_1\to\infty}\frac{1}{M_1}\mathbf{h}_{j'j'k1}^H\mathbf{h}_{j'j'k'1} \\ &= \eta\delta(k'-k), \end{aligned}$$

and

$$\begin{aligned} \lim_{M\to\infty}\frac{1}{M}\mathbf{h}_{j'j'k2}^H\mathbf{h}_{j'j'k'2} &= \frac{M_2}{M}\lim_{M_2\to\infty}\frac{1}{M_2}\mathbf{h}_{j'j'k2}^H\mathbf{h}_{j'j'k'2} \\ &= (1-\eta)\delta(k'-k). \end{aligned}$$

Therefore, we can get

$$\begin{aligned} &\lim_{M\to\infty}\frac{1}{M}\mathbf{h}_{j'j'k}^H\mathbf{h}_{j'j'k'} \\ &= (\eta\alpha_{j'j'k}^2(\theta_1) + (1-\eta)\alpha_{j'j'k}^2(\theta_2))\delta(k'-k). \end{aligned}$$

Finally, we can get the result as

$$\begin{aligned} \lim_{M\to\infty}\frac{1}{M}\mathbf{H}_{j'j'}^H\mathbf{H}_{j'j'} &= \mathrm{diag}\left\{\eta\alpha_{j'j'1}^2(\theta_1) + (1-\eta)\right. \\ &\left.\times\alpha_{j'j'1}^2(\theta_2), \cdots, \eta\alpha_{j'j'K}^2(\theta_1) + (1-\eta)\alpha_{j'j'K}^2(\theta_2)\right\}. \end{aligned} \tag{16}$$

2) For $\mathbf{h}_{j'jk}^H\mathbf{H}_{j'j'}$, we have

$$\begin{aligned} &\mathbf{h}_{j'jk}^H\mathbf{h}_{j'j'k'} \\ &= \begin{bmatrix} \alpha_{j'jk}(\theta_1)\mathbf{h}_{j'jk1} \\ \alpha_{j'jk}(\theta_2)\mathbf{h}_{j'jk2} \end{bmatrix}^H \begin{bmatrix} \alpha_{j'j'k'}(\theta_1)\mathbf{h}_{j'j'k'1} \\ \alpha_{j'j'k'}(\theta_2)\mathbf{h}_{j'j'k'2} \end{bmatrix} \\ &= \alpha_{j'jk}^*(\theta_1)\alpha_{j'j'k'}(\theta_1)\mathbf{h}_{j'jk1}^H\mathbf{h}_{j'j'k'1} \\ &\quad + \alpha_{j'jk}^*(\theta_2)\alpha_{j'j'k'}(\theta_2)\mathbf{h}_{j'jk2}^H\mathbf{h}_{j'j'k'2}. \end{aligned}$$

$$\gamma_{jk}(\theta_1,\theta_2)=\frac{\mathbb{E}\{\left|\sqrt{\rho_j}\mathbf{h}_{jjk}^H[\mathbf{F}_j]_k[\mathbf{d}_j]_k\right|^2\}}{\sigma_{\mathrm{n}}^2+\mathbb{E}\{\sum\limits_{k'\neq k}\left|\sqrt{\rho_j}\mathbf{h}_{jjk'}^H[\mathbf{F}_j]_{k'}[\mathbf{d}_j]_{k'}\right|^2\}+\mathbb{E}\{\sum\limits_{j'\neq j}\left|\sqrt{\rho_{j'}}\mathbf{h}_{j'jk}^H\mathbf{F}_{j'}\mathbf{d}_{j'}\right|^2\}}. \tag{9}$$

When the number of antennas tends to infinity, for $\mathbf{h}_{j'jk1}^H\mathbf{h}_{j'j'k'1}$ and $\mathbf{h}_{j'jk2}^H\mathbf{h}_{j'j'k'2}$, we have

$$\lim_{M\to\infty}\frac{1}{M}\mathbf{h}_{j'jk1}^H\mathbf{h}_{j'j'k'1}=\eta\lim_{M_1\to\infty}\frac{1}{M_1}\mathbf{h}_{j'jk1}^H\mathbf{h}_{j'j'k'1}=0.$$

Similarly,

$$\lim_{M\to\infty}\frac{1}{M}\mathbf{h}_{j'jk2}^H\mathbf{h}_{j'j'k'2}=(1-\eta)\lim_{M_2\to\infty}\frac{1}{M_2}\mathbf{h}_{j'jk2}^H\mathbf{h}_{j'j'k'2}=0.$$

Then we can know that

$$\lim_{M\to\infty}\frac{1}{M}\mathbf{h}_{j'jk}^H\mathbf{H}_{j'j'}=0. \tag{17}$$

According to (16) and (17), we can write (14) as (15). ■

B. Analysis of the signal power

Our goal is to find a set of θ_1 and θ_2 that satisfy (11), for which we need a set of θ_1 and θ_2 that maximize (15), thus we need to obtain the expression of ρ_j through the analysis of the signal power P_j.

According to the (6), we have

$$\begin{aligned}P_j &= \mathbb{E}\left\{\|\mathbf{s}_j\|^2\right\}\\ &= \rho_j\mathbb{E}\left\{\|(\mathbf{F}_j\mathbf{d}_j)\|^2\right\}\\ &= \rho_j\mathrm{Tr}(\mathbf{F}_j\mathbf{F}_j^H) \qquad (18)\\ &= \rho_j\mathrm{Tr}(\left(\mathbf{H}_{jj}^H\mathbf{H}_{jj}\right)^{-1})\\ &= \sum_{k=1}^{K}\frac{\rho_j}{M_1\alpha_{jjk}^2(\theta_1)+M_2\alpha_{jjk}^2(\theta_2)}, \qquad (19)\end{aligned}$$

where substituting (4) can get the second equation, substituting (5) can get the third equation, substituting (12) and (16) can get the last two equations, respectively.

C. Throughput with the perfect CSI

By substituting (19) into (15), we can obtain the SINR for the k-th user of the j-th cell as

$$\bar{\gamma}_{jk}(\theta_1,\theta_2)=\frac{P_j}{\sum\limits_{k'=1}^{K}\frac{\sigma_{\mathrm{n}}^2}{M_1\alpha_{jjk'}^2(\theta_1)+M_2\alpha_{jjk'}^2(\theta_2)}}. \tag{20}$$

Thus, according to (10), the corresponding throughput for the all K users in the j-th cell can be expressed as

$$\begin{aligned}&\bar{R}_j(\theta_1,\theta_2)\\ &=K\mathbb{E}\left\{\log_2\left(1+\frac{P_j}{\sum\limits_{k'=1}^{K}\frac{\sigma_{\mathrm{n}}^2}{M_1\alpha_{jjk'}^2(\theta_1)+M_2\alpha_{jjk'}^2(\theta_2)}}\right)\right\}. \qquad (21)\end{aligned}$$

In the case of the limit of the number of BS antennas, we use $\bar{R}_j(\theta_1,\theta_2)$ instead of $R_j(\theta_1,\theta_2)$, i.e., our goal is becoming to maximize the value of $\bar{R}_j(\theta_1,\theta_2)$. Therefore, we next propose a lemma to simplify (21).

Lemma 2. *Assume that the users are in the same uniform distribution, we have*

$$\bar{R}_j(\theta_1,\theta_2)\geqslant\tilde{R}_j(\theta_1,\theta_2)=K\log_2\left(1+\frac{P_j}{\sigma_{\mathrm{n}}^2 f(\theta_1,\theta_2)}\right), \tag{22}$$

where

$$\begin{aligned}f(\theta_1,\theta_2)=&\iint\frac{K}{M_1\alpha_{jjk'}^2(\theta_1)+M_2\alpha_{jjk'}^2(\theta_2)}\\ &\times g(\phi_{jjk'})h(\theta_{jjk'})d(\phi_{jjk'})d(\theta_{jjk'}),\end{aligned}$$

$g(\phi_{jjk'})$ and $h(\theta_{jjk'})$ are the probability density functions (PDFs) of $\phi_{jjk'}$ and $\theta_{jjk'}$, respectively. Moreover, they are defined as

$$g(\phi_{jjk'})=\begin{cases}\frac{3}{2\pi}, & -\frac{\pi}{3}\leqslant\phi_{jjk'}\leqslant\frac{\pi}{3},\\ 0, & \text{else},\end{cases}$$

$$h(\theta_{jjk'})=\frac{2h_{\mathrm{BS}}^2}{r_1^2-r_2^2}\cot(\theta_{jjk'})(1+\cot^2(\theta_{jjk'}))$$

for $\arctan(h_{\mathrm{BS}}/r_1)\leqslant\theta_{jjk'}\leqslant\arctan(h_{\mathrm{BS}}/r_2)$ *and* $h(\theta_{jjk'})=0$ *otherwise.*

Proof: Through simple algebra calculations, we know that the log-function in (21) is a convex function. Then the lower bound of (21) is obtained with the help of Jensen's inequality:

$$\begin{aligned}&\bar{R}_j(\theta_1,\theta_2)\geqslant\tilde{R}_j(\theta_1,\theta_2)\\ &=K\log_2\left(1+\frac{P_j}{E\left\{\sum\limits_{k'=1}^{K}\frac{\sigma_{\mathrm{n}}^2}{M_1\alpha_{jjk'}^2(\theta_1)+M_2\alpha_{jjk'}^2(\theta_2)}\right\}}\right).\end{aligned}$$

Since the users are in the same uniform distribution, we have (22).

According to our system model and Fig. 1, we know that $g(\phi_{jjk'})$ is subject to uniform distribution, i.e.,

$$g(\phi_{jjk'})=\begin{cases}\frac{3}{2\pi}, & -\frac{\pi}{3}\leqslant\phi_{jjk'}\leqslant\frac{\pi}{3},\\ 0, & \text{else}.\end{cases} \tag{23}$$

Denote the distance from the k'-th user in the j-th cell to the foot of the j-th BS as $r_{jjk'}$, then according to Fig. 1, we have

$$r_{jjk'}=h_{\mathrm{BS}}\cot\theta_{jjk'}.$$

In addition, with the uniform distribution of the users, we can get the PDF of $r_{jjk'}$ as

$$h_r(r_{jjk'})=\begin{cases}\frac{2}{r_1^2-r_2^2}r_{jjk'}, & r_2\leqslant r_{jjk'}\leqslant r_1,\\ 0, & \text{else}.\end{cases}$$

Hence, we have

$$h(\theta_{jjk'}) = h_r(r_{jjk'}) \left| r'_{jjk'} \right|,$$

which means

$$h(\theta_{jjk'}) = \frac{2h_{\mathrm{BS}}^2}{r_1^2 - r_2^2} \cot(\theta_{jjk'})(1 + \cot^2(\theta_{jjk'})) \tag{24}$$

for $\arctan(h_{\mathrm{BS}}/r_1) \leqslant \theta_{jjk'} \leqslant \arctan(h_{\mathrm{BS}}/r_2)$ and $h(\theta_{jjk'}) = 0$ otherwise. ∎

With the throughput in (22), we can optimize $\tilde{R}_j(\theta_1, \theta_2)$ to design the tilts, i.e., (11) can be approximately achieved with

$$\max_{\theta_1, \theta_2} \tilde{R}_j(\theta_1, \theta_2). \tag{25}$$

Then, we can use the exhaustive search to find the two tilts θ_1 and θ_2.

IV. Optimization for the Imperfect CSI

In this section, optimization for the imperfect CSI is investigated. We first analyze the channel estimation performance. Then, we get the expression of the SINR and analyze the signal power. Finally, we obtain the two optimal tilts by maximizing the approximated throughput.

A. Channel estimation

During a dedicated uplink training phase, the K users in each cell transmit mutually orthogonal pilot sequences which allow the BSs to compute estimete $\hat{\mathbf{H}}_{jj}$ of their local channels $\mathbf{H}_{jj}$. As the length of pilots is limited in the block fading scenario, the same set of orthogonal pilot sequences is reused in every cell to avoid intra-cell interference, and the channel estimate is corrupted by the ICI. We assume that noise in the channel estimation can be ignored, and it can be applied to both low and high transmission SNR. Since the number of BS antennas is large, high SNR can be obtained at the user when the transmission SNR is low. Thus, the impact of noise is relatively smaller than the interference and can be ignored. Thus, we have the channel estimate as

$$\hat{\mathbf{H}}_{jj} = \mathbf{H}_{jj} + \sum_{j' \neq j} \mathbf{H}_{jj'}, \tag{26}$$

where $\mathbf{H}_{jj'}$ indicates the channel matrix of the j'-th cell to the j-BS. Then, according to (12), we have

$$\mathbf{F}_j = \hat{\mathbf{H}}_{jj} \left(\hat{\mathbf{H}}_{jj}^H \hat{\mathbf{H}}_{jj} \right)^{-1}. \tag{27}$$

The received signal y_{jk} of the k-th user in the j-th cell is given as (8), we now further process the first three items of it:

1) For the first two items, we can analyze with $\mathbf{h}_{jjk}^H \mathbf{F}_j$. Substitute (26) and (27) into $\mathbf{h}_{jjk}^H \mathbf{F}_j$, we have

$$\begin{aligned} &\lim_{M\to\infty} \mathbf{h}_{jjk}^H \mathbf{F}_j \\ &= \lim_{M\to\infty} \mathbf{h}_{jjk}^H \hat{\mathbf{H}}_{jj} \left(\hat{\mathbf{H}}_{jj}^H \hat{\mathbf{H}}_{jj} + \sum_{j' \neq j} \sum_{i' \neq j} \hat{\mathbf{H}}_{jj'}^H \hat{\mathbf{H}}_{ji'} \right)^{-1}. \end{aligned} \tag{28}$$

According to the proof of Lemma 1, we can get

$$\begin{aligned} &\lim_{M\to\infty} \frac{1}{M} \mathbf{h}_{jjk}^H \hat{\mathbf{H}}_{jj} = \left(\eta \alpha_{jjk}^2(\theta_1) + (1-\eta)\alpha_{jjk}^2(\theta_2) \right) \mathbf{e}_k, \\ &\lim_{M\to\infty} \frac{1}{M} \hat{\mathbf{H}}_{jj}^H \hat{\mathbf{H}}_{jj} = \mathrm{diag}(\eta \alpha_{jj1}^2(\theta_1) + (1-\eta) \\ &\times \alpha_{jj1}^2(\theta_2), \cdots, \eta \alpha_{jjK}^2(\theta_1) + (1-\eta)\alpha_{jjK}^2(\theta_2)), \end{aligned} \tag{29}$$

$$\begin{aligned} &\lim_{M\to\infty} \frac{1}{M} \sum_{j' \neq j} \sum_{i' \neq j} \hat{\mathbf{H}}_{jj'}^H \hat{\mathbf{H}}_{ji'} = \\ &\mathrm{diag} \left(\sum_{j' \neq j} \left(\eta \alpha_{jj'1}^2(\theta_1) + (1-\eta)\alpha_{jj'1}^2(\theta_2) \right), \cdots, \right. \\ &\left. \sum_{j' \neq j} \left(\eta \alpha_{jj'K}^2(\theta_1) + (1-\eta)\alpha_{jj'K}^2(\theta_2) \right) \right). \end{aligned} \tag{30}$$

Then, the first two items of (8) can be written as

$$\begin{aligned} &\lim_{M\to\infty} \mathbf{h}_{jjk}^H [\mathbf{F}_j]_k \\ &= \frac{M_1 \alpha_{jjk}^2 + M_2 \alpha_{jjk}^2(\theta_2)}{M_1 \sum_{j'=1}^L \alpha_{jj'k}^2(\theta_1) + M_2 \sum_{j'=1}^L \alpha_{jj'k}^2(\theta_2)}, \end{aligned} \tag{31}$$

$$\lim_{M\to\infty} \mathbf{h}_{jjk}^H [\mathbf{F}_j]_{k'} = 0, k' \neq k. \tag{32}$$

2) For the third item $\mathbf{h}_{j'jk}^H \mathbf{F}_{j'}$, we have

$$\begin{aligned} &\lim_{M\to\infty} \mathbf{h}_{j'jk}^H \mathbf{F}_{j'} = \lim_{M\to\infty} \mathbf{h}_{j'jk}^H \hat{\mathbf{H}}_{j'j'} \\ &\times \left(\hat{\mathbf{H}}_{j'j'}^H \hat{\mathbf{H}}_{j'j'} + \sum_{j'' \neq j'} \sum_{i'' \neq j'} \hat{\mathbf{H}}_{j'j''}^H \hat{\mathbf{H}}_{j'i''} \right)^{-1}. \end{aligned} \tag{33}$$

Then, according to the proof of Lemma 1, we take the limit for each item of the above formula and have

$$\begin{aligned} &\lim_{M\to\infty} \frac{1}{M} \sum_{j'' \neq j'} \mathbf{h}_{j'jk}^H \hat{\mathbf{H}}_{j'j'} = \\ &\left(\eta \alpha_{j'jk}^2(\theta_1) + (1-\eta)\alpha_{j'jk}^2(\theta_2) \right) \mathbf{e}_k. \end{aligned} \tag{34}$$

For the limit of the inverse in (33), the results in (29) and (30) can be employed. Substituting (29), (30), and (34) into (33), we can get

$$\begin{aligned} &\lim_{M\to\infty} \mathbf{h}_{j'jk}^H \mathbf{F}_{j'} \\ &= \frac{M_1 \alpha_{j'jk}^2(\theta_1) + M_2 \alpha_{j'jk}^2(\theta_2)}{M_1 \sum_{j''=1}^L \alpha_{j'j''k}^2(\theta_1) + M_2 \sum_{j''=1}^L \alpha_{j'j''k}^2(\theta_2)} \mathbf{e}_k. \end{aligned} \tag{35}$$

B. Analysis of the SINR

Substituting (5) and (9), the SINR of the k-th user in the j-th cell is given by

$$\begin{aligned} &\gamma_{jk}(\theta_1, \theta_2) \\ &= \frac{\left| \sqrt{\rho_j} \mathbf{h}_{jjk}^H [\mathbf{F}_j]_k \right|^2}{\sum_{k' \neq k} \left| \sqrt{\rho_j} \mathbf{h}_{jjk}^H [\mathbf{F}_j]_{k'} \right|^2 + \sum_{j' \neq j} \left\| \sqrt{\rho_{j'}} \mathbf{h}_{j'jk}^H \mathbf{F}_{j'} \right\|^2 + \sigma_{\mathrm{n}}^2}. \end{aligned} \tag{36}$$

Then, substituting (31), (32), and (35) into (36), we have (37).

For further simplification, we will get the expressions of ρ_j and $\rho_{j'}$ through P_j and $P_{j'}$. Next, we will make a relevant derivation of P_j.

$$\check{\gamma}_{jk}(\theta_1,\theta_2)=\lim_{M\to\infty}\gamma_{jk}(\theta_1,\theta_2)=\frac{\left|\frac{M_1\alpha_{jjk}^2+M_2\alpha_{jjk}^2(\theta_2)}{M_1\sum_{j'=1}^{L}\alpha_{jj'k}^2(\theta_1)+M_2\sum_{j'=1}^{L}\alpha_{jj'k}^2(\theta_2)}\right|^2\rho_j}{\sum_{j'\neq j}\left|\frac{M_1\alpha_{j'jk}^2(\theta_1)+M_2\alpha_{j'jk}^2(\theta_2)}{M_1\sum_{j''=1}^{L}\alpha_{j'j''k}^2(\theta_1)+M_2\sum_{j''=1}^{L}\alpha_{j'j''k}^2(\theta_2)}\right|^2\rho_{j'}+\sigma_{\mathrm{n}}^2}. \tag{37}$$

C. Analysis of the signal power

Substituting (27) to (18), we have

$$P_j=\rho_j\mathrm{Tr}((\hat{\mathbf{H}}_{jj}^H\hat{\mathbf{H}}_{jj})^{-1}).$$

According to the limits in (29) and (30), we have

$$\lim_{M\to\infty}P_j=\sum_{k=1}^{K}\frac{\rho_j}{M_1\sum_{j'=1}^{L}\alpha_{jj'k}^2(\theta_1)+M_2\sum_{j'=1}^{L}\alpha_{jj'k}^2(\theta_2)}. \tag{38}$$

When substitute (38) into (37), the corresponding throughput is

$$\check{R}_j(\theta_1,\theta_2)=K\mathbb{E}\left\{\log_2\left(1+\check{\gamma}_{jk}(\theta_1,\theta_2)\right)\right\}. \tag{39}$$

Similarly, we only need to optimize $\check{R}_j(\theta_1,\theta_2)$ in (39) to optimize the tilts. i.e., (11) can be approximately achieved with

$$\max_{\theta_1,\theta_2}\ \check{R}_j(\theta_1,\theta_2). \tag{40}$$

Then, we can use the exhaustive search to find the two tilts θ_1 and θ_2.

V. Numerical Results

In this section, the performance of the proposed optimization scheme is evaluated. The antenna parameters are set as $\phi_{3\mathrm{dB}}=70°$, $\theta_{3\mathrm{dB}}=7°$, $SLL_{\mathrm{az}}=25$ dB, $SLL_{\mathrm{el}}=20$ dB, $SLL_{\mathrm{tot}}=25$ dB, and $\alpha_{\max}=0$ dBi. The system parameters are $K=10$, $M=100,\eta=0.5,M_1=50,M_2=50$. The cell radius is $r_1=120$ m and the cell hole radius is $r_2=10$ m, $h_{\mathrm{BS}}=30$ m. The optimized tilts are $\theta_1=0.3142$ rad and $\theta_2=0.55$ rad with the perfect CSI and the imperfect CSI. The large scale fading is composed of the path loss as $\beta_{ljk}=d_{ljk}^{-1.5}$, where d_{ljk} denotes the distance between the k-th user of the j-th cell and the BS of the l-th cell. According to (2) and (7), we can know that β_{ljk} only affects the magnitude of the channel vector. When we calculate the power, it is expressed as $\beta_{ljk}^2=d_{ljk}^{-3}$, i.e., the exponent factor of pathloss over distance is 3. The cell signal-to-noise ratio (SNR) is defined as $10\log_{10}(P_j/\sigma_{\mathrm{n}}^2)-90$ dB, and is 0 dB when it is not the changing variable, and $\sigma_{\mathrm{n}}^2=1$.

We simulate two scenarios with perfect CSI and imperfect CSI, which correspond to Section III and Section IV, respectively. In each scenario, we simulate the relationship between the SNR, the number of the BS antennas M, the number of users K, and the throughput. For the perfect CSI scenario, we show the actual throughput which is obtained by substituting (14) into (10), the limit of the throughput in (21), and the throughput lower bound in (22). For the imperfect CSI scenario, we show the actual throughput which is obtained by substituting (36) into (10) and the limit of the throughput in (39). As a reference, we also compare these throughputs

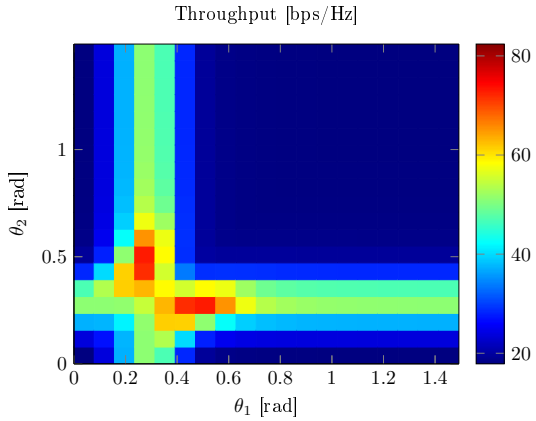

Fig. 2. The throughput versus the tilts θ_1 and θ_2 with the perfect CSI.

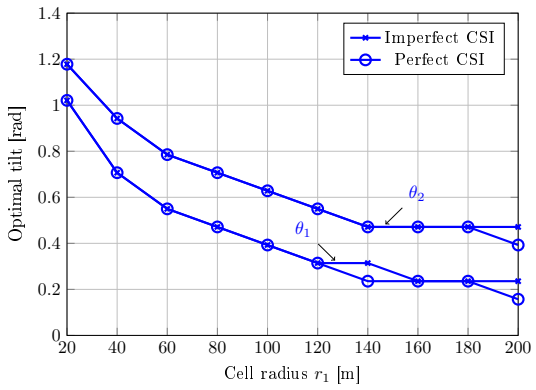

Fig. 3. The optimal tilts versus the cell radius r_1 with the perfect CSI and the imperfect CSI.

with that achieved with typical tilts. On typical tilt set is $\theta_1=\theta_2=0.34$, which means the two tilts point to the center of the cell in that the cellular area is equally divided at this point. This tilt set is named cell-center tilt. Another typical tilt set is $\theta_1=0.2808,\theta_2=0.4571$, which means the cell is divided equally into two parts with the same area, and the two tilts point to the center of each part. This tilt set is named cell-split-center tilt. Additionally, the results with tilt optimization, such as the relationship between the optimal tilts and the cell radius r_1, are also illustrated.

A. Results with tilt optimization

In Fig. 2, the throughput lower bound in (22) versus the two tilts with the perfect CSI is shown. It is observed that large throughput is achieved when one tilt is close to 0.5 rad, which is the tilt that points to the center of the cell. This is because the difference between the antenna tilt and the elevation angle

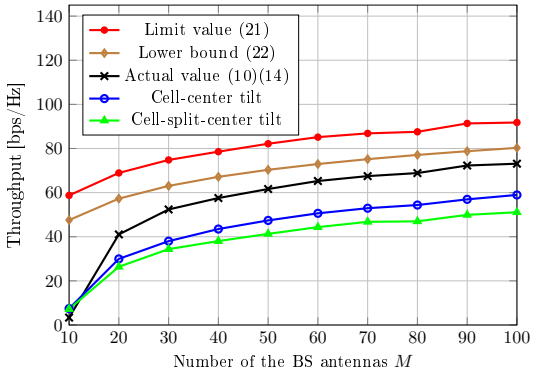

Fig. 4. The throughputs versus the number of BS antennas M with the perfect CSI.

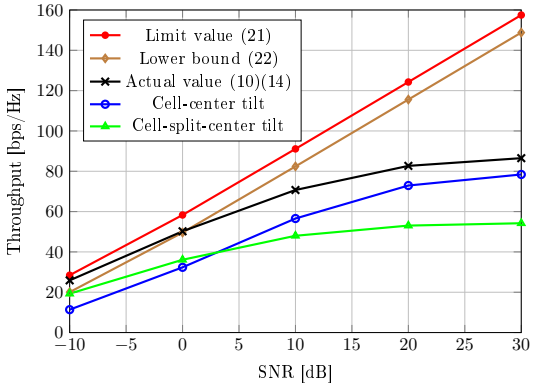

Fig. 5. The throughputs versus the SNR with the perfect CSI.

is small in this case, and the antenna gain is large, cf. (1). The results with the limit of the throughput in (39) versus the two tilts with the imperfect CSI are similar.

In Fig. 3, the two tilts that achieve the maximum throughput with the perfect CSI and the imperfect CSI are shown. First, we can see that the optimized two tilts are not the same. This means that it is beneficial to employ two arrays with two different tilts. Second, we can see that the optimal tilts decrease with the increase of the cell radius. This is because the cell center moves away from the BS, and larger tilts can result into smaller differences between the tilts and the elevation angles, and the antenna gain is higher, cf. (1). Third, we can see that the tilts with the perfect CSI and the imperfect CSI are almost the same. This means we can use the same optimized tilts in the two scenarios with negligible performance penalty.

B. Results with the perfect CSI

In this scenario, we compare the performance of three different expressions: 1) the actual value of the throughput obtained by substituting (14) into (10); 2) the limit value of the throughput (21); 3) the lower bound expression (22) of the throughput in Lemma 2. Additionally, we compare the actual throughputs with the reference tilts mentioned in the beginning of this section.

Fig. 4 shows the curves of the throughputs of the three expressions and the reference methods versus the number of

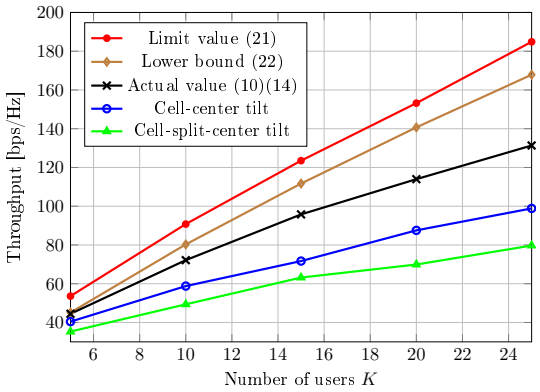

Fig. 6. The throughputs versus the number of users K with the perfect CSI.

the BS antennas M. It is observed that all the throughputs are increasing in the same trend. First, we can see the lower bound is always lower than the limit value and is close to the limit value, which verifies that the derived lower bound is effective. Second, we can see that the actual value is close to the lower bound, which means it is effective to employ the lower bound to optimize the tilts. Third, we can see that the two reference tilts are of lower throughputs than the optimized tilts. This verifies that the proposed tilt design is effective. Forth, we can see that the actual throughput will approach the limit throughput when M gradually increases from $M = 10$. However, there will still be residual interference, i.e., the interference cannot reach zero as (17). This is because M is limited in the simulations and the decreasing of interference in (17) gets slow as M increases.

Fig. 5 shows the curves of the throughputs of the three expressions and the reference methods versus the SNR. First, we can see the limit value and the lower bound value are increasing in the same trend and the lower bound value is slightly lower. These results verify the analysis results of the throughputs with perfect CSI in that the SINR increases with the SNR, cf. (21) and (22). Second, the actual value saturates with the increase of the SNR and the gap between the actual value and the limit value or the lower bound increases with the increase of the SNR. This is because the limit value and lower bound are derived in the limit of the number of the BS antennas and the interference is eliminated in this asymptotic region, but the actual value are obtained with limit number of BS antennas and the interference always exists. Third, the actual value is larger than the throughputs obtained with the reference tilts, which again shows the superiority of the optimized tilts.

Fig. 6 shows the curves of the throughputs of the three expressions and the reference methods versus the number of users K. It can be seen that all the throughputs are increasing but with different slopes. First, the limit value and the lower bound increase in the same slope, which means the derived bound is effective with the number of users changing. The gap between the lower bound and the actual value increases as the number of users increases, which is because the interference becomes more severe as the number of users increases and the interference is eliminated in the asymptotic region. Addi-

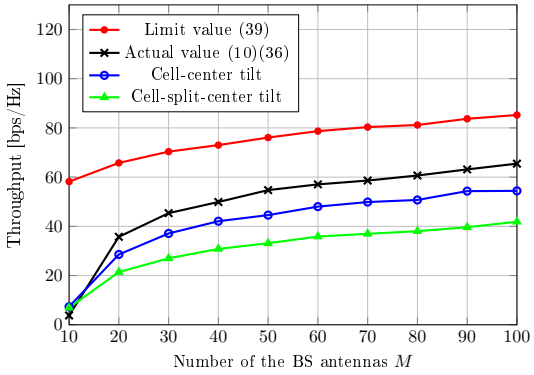

Fig. 7. The throughputs versus the number of BS antennas M with the imperfect CSI.

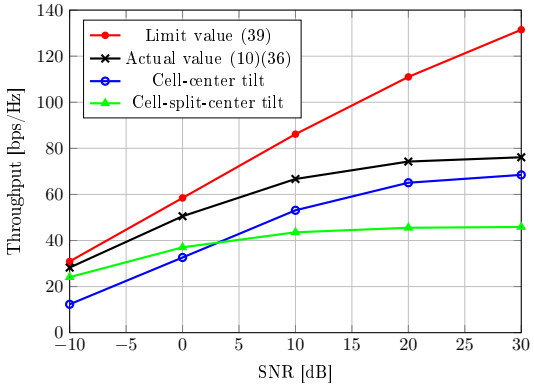

Fig. 8. The throughputs versus the SNR with the imperfect CSI.

tionally, we can see that the gap between the actual value and the throughputs of the two reference tilts are also increasing with the increase of the number of users. This means that the proposed tilt design is effective in mitigating interference when the number of users is large.

C. Results with the imperfect CSI

In this scenario, we compare the actual value obtained by substituting (36) into (10) and the limit value in (39) of the throughput. Moreover, the throughputs with the reference tilts are also compared.

Fig. 7 shows the curves of the throughputs of the two expressions and the reference tilts versus the number of the number of BS antennas M. Similar to the perfect CSI scenarios, the limit value is close to the actual value and the increase in the same trend. Additionally, the optimized tilts can achieve higher throughputs than the two reference tilts. Thus, the proposed tilt optimization is also effective in the imperfect CSI scenario.

Fig. 8 shows the curves of the throughputs of the two expressions and the reference tilts versus the SNR. Similar to the perfect CSI scenario, the gap between the actual value and the limit value increases as the SNR increase, which is because the intra-cell interference is eliminated in the asymptotic region, i.e., the actual value is influence by both the intra-cell interference and the ICI, but the limit value is only

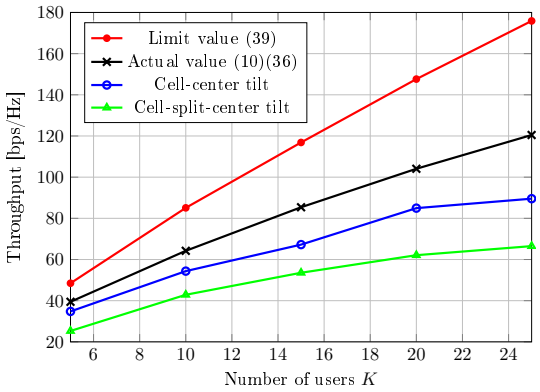

Fig. 9. The throughputs versus the number of users K with the imperfect CSI.

influenced by the ICI. Moreover, we can see that the optimized tilts can achieve higher throughputs than the reference tilts.

Fig. 9 shows the curves of the throughputs of the two expressions and the reference tilts versus the number of users K. Similar to the perfect CSI scenarios, the gap between the limit value and the actual value increases with the increase of the number of users, and the reason is that the intra-cell interference is eliminated in the asymptotic region. Additionally, the superiority of the optimized tilts than the two reference tilts is more evident when the number of users increases. Thus, the proposed tilt optimization is effective in mitigating interference in the imperfect CSI scenario when the number of users is large.

VI. Conclusions

In this paper, we analyze the asymptotic expression of the throughput for the multi-cell massive MIMO system with two tilts. Two scenarios with the perfect CSI and the imperfect CSI are considered, and the two optimal tilts are obtained by maximizing the throughput expression. Then, we get the relationship between the optimal tilts and the cell radius, and the relationship between the throughput and the SNR and the number of the BS antennas with simulations, which show that the designed tilts are useful in increasing the system throughput.

Funding

This research was supported by Project LY20F010007 supported by Zhejiang Provincial Natural Science Foundation of China and Project 61601152 and Project U1609216 supported by National Natural Science Foundation of China.

References

[1] L. Lu, G. Y. Li, A. L. Swindlehurst, A. Ashikhmin, and R. Zhang, "An overview of massive MIMO: Benefits and challenges," *IEEE J. Sel. Topics Signal Process.*, vol. 8, no. 5, pp. 742–758, Oct. 2014.

[2] H. Huh, G. Caire, H. Papadopoulos, and S. Ramprashad, "Achieving "massive MIMO" spectral efficiency with a not-solarge number of antennas," *IEEE Trans. Wireless Commun.*, vol. 11, no. 9, pp. 3226–3239, Sep. 2012.

[3] H. Yin, D. Gesbert, M. Filippou, and Y. Liu, "A coordinated approach to channel estimation in large-scale multipleantenna systems," *IEEE J. Sel. Areas Commun.*, vol. 31, no. 2, pp. 264–273, Feb. 2013.

[4] N. Seifi, M. Coldrey, and M. Viberg, "Throughput optimization for MISO interference channels via coordinated user-specific tilting," *IEEE Commun. Lett.*, vol. 16, no. 8, pp. 1248–1251, Aug. 2012.

[5] N. Seifi, R. W. Heath, M. Coldrey, and T. Svensson, "Joint transmission mode and tilt adaptation in coordinated small-cell networks," in *Proc. IEEE Intern. Conf. Commun. Works. (ICC)*, Sydney, Australia, Jun. 2014, pp. 598–603.

[6] W. Lee, S. R. Lee, H. B. Kong, S. Lee, and I. Lee, "Downlink vertical beamforming designs for active antenna systems," *IEEE Trans. Commun.*, vol. 62, no. 6, pp. 1897–1907, Jun. 2014.

[7] W. Guo, J. Fan, G. Y. Li, Q. Yin, X. Zhu, and Y. Fu, "MIMO transmission with vertical sectorization for LTE-A downlink," *IEEE Wireless Commun. Lett.*, vol. 5, no. 4, pp. 372–375, Aug. 2016.

[8] A. Hu, "Antenna tilt adaptation for multi-cell massive MIMO systems," *IEEE Commun. Lett.*, vol. 21, no. 11, pp. 2436–2439, Nov. 2017.

[9] W. Lee, S. R. Lee, H. B. Kong, and I. Lee, "3D beamforming designs for single user MISO systems," in *Proc. IEEE Global Commun. Conf. (GLOBECOM)*, Atlanta, USA, Dec. 2013, pp. 9–13.

[10] J. Koppenborg, H. Halbauer, S. Saur, and C. Hoek, "3D beamforming trials with an active antenna array," in *Proc. Int. ITG Workshop Smart Antennas*, Dresden, Germany, Mar. 2012, pp. 110–114.

[11] N. Seifi, J. Zhang, R. W. Heath, T. Svensson, and M. Coldrey, "Coordinated 3D beamforming for interference management in cellular networks," *IEEE Trans. Wireless Commun.*, vol. 13, no. 10, pp. 5396–5410, Oct. 2014.

[12] 3GPP TR 36.814 V9.0, "Further advancements for E-UTRA physical layer aspects," *Tech. Rep.*, Mar. 2010.

[13] J. Hoydis, S. ten Brink, and M. Debbah, "Massive MIMO in the UL/DL of cellular networks: How many antennas do we need?" *IEEE J. Sel. Areas Commun.*, vol. 31, no. 2, pp. 160–171, Feb. 2013.